Article:

eprints@whiterose.ac.uk
https://eprints.whiterose.ac.uk/

Novel water-assisting low firing MoO₃ microwave dielectric ceramics

Di Zhou[*a,b], Li-Xia Pang[a,c], Da-Wei Wang[a], & Ian M. Reaney[*a]

[a]Department of Materials Science and Engineering, University of Sheffield, S1 3JD,
UK

[b]Electronic Materials Research Laboratory, Key Laboratory of the Ministry of
Education & International Center for Dielectric Research, School of Electronic and
Information Engineering, Xi'an Jiaotong University, Xi'an 710049, China

[c]Micro-optoelectronic Systems Laboratories, Xi'an Technological University, Xi'an
710032, Shaanxi, China

[*]Corresponding author E-mail address: zhoudi1220@gmail.com (Di Zhou) & i.m.reaney@sheffield.ac.uk (Ian M.
Reaney)

Abstract

MoO_3 ceramics can not be well densified via conventional solid state method and a low relative density (ρ) was obtained (~ 64.5 % at 680 $^{\circ}$C) with a permittivity (ε_r) ~ 7.58, a quality factor (Qf) ~ 35,000 GHz and a temperature coefficient of resonant frequency ~ − 39 ppm/$^{\circ}$C. However, cold sintering at 150 $^{\circ}$C using 4 wt. % H_2O at 150 MPa enhanced densification and give a ρ ~ 76.8 % and ε_r ~ 8.31 but with a Qf of only ~ 900 GHz. The addition of $(NH_4)_6Mo_7O_{24} \cdot 4H_2O$ further improved densification to give a ρ ~ 83.7 % after annealing at 700 $^{\circ}$C, resulting in a ε_r ~ 9.91 with a Qf ~ 11,800 GHz. We conclude that partially water-soluble oxides may benefit from cold sintering but despite the higher density, lower Qf cannot be avoided due to the impurities and grain boundary phases.

Keywords: (Ceramics, Microwave Dielectrics)

Introduction

Low temperature co-fired ceramic (LTCC) technology has become an important fabrication method for modern electronic devices due the low cost of manufacture and potential of the integration multiple microwave (MW) circuits.[1-4] LTCCs are required to have lower sintering temperatures than that of the inner metal electrodes (typically Ag, 961 °C)[5,6] but classic MW dielectric ceramics typically densify at > 1000 °C.[1-7] Lowering the sintering temperature of a MW ceramic by the addition of low-melting-point glasses and oxides has been used to fabricate many commercial LTCCs.[1-7] The search for intrinsically low sintering temperature LTCC has accelerated in recent years and the so-called family of ultra-LTCC (ULTCC) compounds can be well sintered at as low as 400 °C.[8-11] Most MW dielectric ceramics are oxides and their sintering temperatures are, to a simple approximation, determined by their melting points. Consequently, systems rich in low melting temperature oxides, such as TeO_2 (733°C), MoO_3 (795°C), Bi_2O_3 (817°C), B_2O_3 (450°C), P_2O_5 (340°C) and V_2O_5 (690°C), have been explored in the past decade.[7-14]

Despite more than 50 types ULTCC molybdates have been reported to date,[8,10,12,14] the understanding of some simple binary compositions, such as MoO_3, is quite limited. MoO_3 powders are usually produced by roasting molybdenum disulfide in industry and take on a yellow color with a monoclinic crystal structure (space group Pbnm, a = 3.962 Å, b = 13.855 Å and c = 3.696Å).[15,16] Its theoretical density ρ is 4.692 g/cm^3 with a melting point 795 °C and many MoO_3-rich compounds have commensurately low melting points and sintering temperatures. However, when not alloyed with other binary compounds, MoO_3 can be well densified.[10,14] Even MoO_3-rich phases in well known phase diagrams, such as the Bi_2O_3-MoO_3 binary system, struggle to achieve

high density,[10] e.g. $Bi_2Mo_3O_{12}$ which, despite its excellent MW properties ($\varepsilon_r \sim 19$, Qf $\sim 21,800$ GHz and TCF ~ -215 ppm/°C), has never been synthesized with relative $\rho > 90$ %. However, Varghese et al.[13] have reported that MoO_3 sintered at 650 °C has a $\varepsilon_r \sim 6.6$ and a Qf $\sim 41,000$ GHz at 11.3 GHz and claimed a high relative ρ ($\sim 88\%$) was achieved via traditional sintering.

Most ceramics are processed using a conventional solid-state method using dry powders at high temperature. However, the poor sinterability of MoO_3 and its partial solubility in water suggest that a solution assisted method, i.e. cold sintering,[17,18] may be beneficial in achieving high ρ. Cold sintering can be explained as a room temperature crystallization or condensation from supersaturated solutions at grain boundaries, which has been employed in salt manufacture for more than one thousand years. The first successful microwave dielectric ceramic densified using cold sintering was Li_2MoO_4.[19,20] The properties of Li_2MoO_4 conventionally sintered at 540 °C were first reported in our previous work[14] with a $\varepsilon_r \sim 5.5$, a Qf $\sim 46,000$ GHz and a TCF ~ -160 ppm/°C. In 2014, Jantunen et al.[19] demonstrated that dense Li_2MoO_4 ceramic may be obtained at 80 °C if water is added. They also recognized that this approach permits the formation of Li_2MoO_4-rich composite ceramics, such as Li_2MoO_4-TiO_2, Li_2MoO_4-$BaTiO_3$ etc.[19-21] In 2016, Randall and his co-workers expanded this natural mechanism to other partially water-soluble MoO_3 and V_2O_5 based systems.[17,18] Solubility in water determines whether a material is suitable for cold sintering. Generally speaking, the cold sintering process (CSP) is a protocol for achieving dense ceramic solids by integrating particles, particle-fluid interface control and external pressure at very low temperatures. CSP uses a transient aqueous environment to achieve densification through a mediated dissolution-precipitation process. Although MoO_3 is only slightly water soluble, ammonium molybdate is highly soluble and

decomposes to MoO_3 and NH_3 (g) above 370 °C.[22,23] Hence, it may be an ideal accelerant for cold sintering of MoO_3 ceramics.

In the present work, a comparison is made between MoO_3 ceramics prepared via a conventional solid-state method and cold sintering using water / $(NH_4)_6Mo_7O_{24} \cdot 4H_2O$ additions. Their phase evolution, microstructure and MW dielectric properties are presented and discussed in detail.

Experimental Section

Solid state reaction method: MoO_3 (> 99%, Fisher Scientific) were ball-milled for 24 h in isopropanol with ZrO_2 balls. After drying, the powders were pressed into cylinders (20 mm in diameter and 4 ~ 5 mm in height) at 30 ~ 50 MPa. Samples were sintered 2 h at 640 to 740 °C.

Cold sintering method: Fine MoO_3 powder was mixed with 4 wt. % water using an agate mortar. The mixture was pressed into cylinders (20 mm in diameter and 4 ~ 5 mm in height) at 100 ~ 150 MPa at 120 ~ 150 °C from 10 min to 30 min. Besides, 10 wt. % $(NH_4)_6Mo_7O_{24} \cdot 4H_2O$ was also mixed with MoO_3 powders and water (4 wt. %) and the same cold sintering process was carried out. To prevent the reaction between MoO3 and the steel, thin PTFE pellets were added inside the die during the cold sintering process. After cold sintering, the samples were dried at 120 °C for 24 h before measurements. Some samples were also annealed at 600 to 700 °C in air after cold sintering.

Structural, Microstructure and Electrical Characterization: Bulk density ρ was measured by the Archimedes' method (using ethanol as liquid) as well as by calculating the mass / volume from basic geometry. X-ray diffraction (XRD) was performed using with Cu Kα radiation (Bruker D2 Phaser) from 5 - 65° 2θ at a step

size of 0.02 °. Natural and fractured surfaces were observed by scanning electron microscopy (SEM, FEI, Inspect F). Dielectric properties at MW frequency were measured using the $TE_{01\delta}$ dielectric resonator method with a network analyzer (Advantest R3767CH; Advantest, Tokyo, Japan) and a home-made heating system. The temperature coefficient of resonant frequency TCF (τ_f) was calculated with the following formula:

$$TCF(\tau_f) = \frac{f_T - f_{T_0}}{f_{T_0} \times (T - T_0)} \times 10^6 \tag{1}$$

where: f_T and f_{T0} are the $TE_{01\delta}$ resonant frequencies at temperature T and T_0, respectively.

Results and Discussions

MoO₃ prepared via solid state reaction method

Relative ρ, ε_r and Qf of MoO_3 ceramics prepared via solid state reaction method as a function of sintering temperature (640 ~ 740 °C) are shown in Fig. 1a. ε_r increased from 6.75 to 7.58 as sintering temperature increased from 640 °C to 680 °C and then decreased a little bit with further increase in sintering temperature. Qf reached a maximum value of 35,000 GHz at 660 °C and remained almost constant for higher sintering temperatures. TCF was ~ − 39 ppm/°C and therefore the overall MW properties were similar to those reported.[13] Although the properties are attractive for the development of MW ceramics, MoO_3 pellets could not be well densified even at tempertaures close to its melting point, only with a maximum relative ρ ~ 64.5 % at 680 °C. An optical image of an MoO_3 pellet sintered at 680 °C and the schematic of crystal structure are shown in Fig. 1b. The pellet has a green-yellow color, similar to the starting powders. Conversely, some grains are observed which are > 100 μm in

diameter which indicates that grain growth is possible but not uniform throughout the ceramic, resulting in poor mechamical strength and low fracture toughness. All the results suggest MoO_3 can not be well sintered using a conventioanl solid-state method even though high Qf is observed. Moreover, its true ε_r is likely to be far higher than the measured value (~ 7.58).

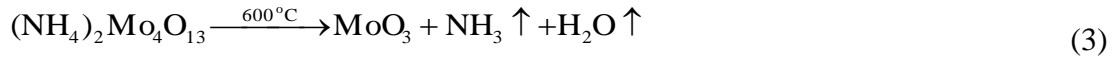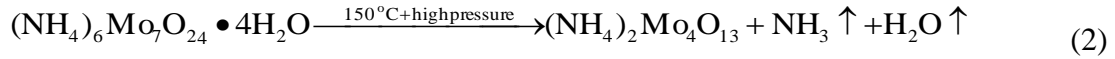**MoO_3 prepared via cold sintering with water only**

XRD patterns of the MoO_3 powders, the natural and fractured surfaces of cold sintered MoO_3 ceramics (sintered 0.5 h at 150 ^oC) and a sample annealed at 620 ^oC are shown in Fig. 2a. Scanning electron and optical images of starting powders and cold sintered MoO_3 ceramics are shown in Fig. 2b. The cold sintered MoO_3 ceramic is black in color on its surface but its interior is deep green. XRD results showed that besides MoO_3, weak peaks of secondary phases were observed on the fracture surface, which indicates that some MoO_3 has reacted with H_2O forming secondary phases that did not decompose after 24 h drying at 150 ^oC. However, due to their low volume fraction they can not be identified. For the natural surface of the cold sintered MoO_3 ceramic, only XRD peaks of MoO_3 phase were observed but with evidence of some preferred orientation. The black surface color is attributed to reduction in the presence of heat, pressure and water. The starting powders adopt an acicular morphology (5 to 10 μm) which is commensurate with an anisotropic crystal structure. The fracture surfaces of cold sintered MoO_3 ceramics show little grain growth compared with the starting powder. The black surface in contrast exhibits bar shaped grains in the a-c plane which are presumably responsible for the increase in intensity of the (020) and (040) peaks with respect to the polycrystalline standard. After annealing above 300 ^oC, both the natural (outer) and fractured (interior) surfaces of cold sintered MoO_3

ceramic returned to the green-yellow color, the same with both that observed in the starting powder and for conventionally sintered MoO_3 ceramic. The relative ρ of MoO_3 ceramic cold sintered at 150 °C was ~ 76.8 % and increased to 77.4 % and 78.7 % at 600 °C and 700 °C, respectively, with an improvement over conventionally sintered MoO_3 as shown in Fig. 3a. When cold sintered ceramics were annealed above 600 °C, large crystal flakes (whiskers) grew from the edge (Fig. 2b), this phenomenon was not observed in conventionally sintered MoO_3 ceramics. Whisker formation is often related to liquid or vapor phase transport and their formation could be driven by the evolution on annealing of H_2O from trapped OH^- groups.[24-26] ε_r and Qf of the cold sintered MoO_3 (150 °C) were ~ 8.31 and ~ 900 GHz but increased to 9.02 and 19,700 GHz, respectively, after annealing at 700 °C as shown in Fig. 3b. TCF value of the cold sintered MoO_3 ceramic is about − 55 ± 15 ppm/°C.

MoO_3 prepared by cold sintering with $(NH_4)_6Mo_7O_{24} \cdot 4H_2O$

Although cold sintering with H_2O improved relative ρ, the optimum value (78.7 %), as shown in Fig. 3a, was below the required density for commercially useful MW ceramics (> 95 %). $(NH_4)_6Mo_7O_{24} \cdot 4H_2O$ is soluble in water and its re-crystallization may enhance densification during cold sintering. Hence, 10 wt. % $(NH_4)_6Mo_7O_{24} \cdot 4H_2O$ was mixed with MoO_3 powders before 4 wt. % H_2O was added. XRD patterns of the $(NH_4)_6Mo_7O_{24} \cdot 4H_2O$ powders, mixtures of MoO_3 ceramic with $(NH_4)_6Mo_7O_{24} \cdot 4H_2O$ cold sintered for 0.5 h at 150 °C and a cold sintered sample annealed at 600 °C are shown in Fig. 4. As reported in literatures, the $(NH_4)_6Mo_7O_{24} \cdot 4H_2O$ decomposes to $(NH_4)_4Mo_5O_{17}$ at ~ 130 °C and the latter decomposes to $(NH_4)_2Mo_4O_{13}$ at about 245 °C.[22,23] In cold sintered MoO_3 (150 °C) sample, $(NH_4)_2Mo_4O_{13}$ phases were revealed in addition to those of the matrix phase

but after annealing at 600 ºC, only MoO_3 phases are observed, suggesting the following reaction sequence:

$$(NH_4)_6Mo_7O_{24} \bullet 4H_2O \xrightarrow{\quad 150\,^\circ C + high\,pressure \quad} (NH_4)_2Mo_4O_{13} + NH_3 \uparrow + H_2O \uparrow \qquad (2)$$

$$(NH_4)_2Mo_4O_{13} \xrightarrow{\quad 600\,^\circ C \quad} MoO_3 + NH_3 \uparrow + H_2O \uparrow \qquad (3)$$

The relative ρ of cold sintered MoO_3 ceramic with $(NH_4)_6Mo_7O_{24} \cdot 4H_2O$ (150 ºC) addition was 82.3 % but the presence of $(NH_4)_2Mo_4O_{13}$ secondary phase affects this value since it has a lower ρ (3.528 g/cm^3)[27] than that of MoO_3 (4.69 g/cm^3) as shown in Fig. 3a. ε_r of cold sintered MoO_3 with $(NH_4)_2Mo_4O_{13}$ as a secondary is ~ 10, larger than that of pure MoO_3. After annealing at 700 ºC, the relative ρ increased to its highest value (83.7 %) but ε_r decreased to 9.91. Qf value of cold sintered MoO_3 with $(NH_4)_6Mo_7O_{24} \cdot 4H_2O$ addition was only 500 GHz, but increased to 11,800 GHz after annealing at 700 ºC. TCF value of the annealed MoO_3 ceramics is about $- 48 \pm 10$ ppm/ºC, which is similar to the conventionally sintered MoO_3 ceramics.

Calculation of ε_r of MoO₃ using Shannon's additive rule

Based on the above results, we conclude that higher relative ρ results in higher ε_r but estimation of the true ε_r of MoO_3 ceramic with high porosity is inaccurate. From Shannon's additive rule,[28] polarizability at microwave region can be treated as the sum of both ionic and electronic components and the molecular polarizability (α) of complex substances maybe estimated by summing α of the constituent:

$$\alpha_{MoO_3} = \alpha_{Mo^{6+}} + 3\alpha_{O^{2-}} = 9.31\,\text{Å}^3, \qquad (4)$$

where the ionic polarizabilities of Mo^{6+} and O^{2-} are 3.28 Å^3 and 2.01 Å^3, respectively.[28,29] Considering the Clausius–Mosotti relation,[30]

$$\varepsilon_{cal} = \frac{3V + 8\pi\alpha}{3V - 4\pi\alpha} \approx 10.96, \tag{5}$$

where V is the cell volume ($202.95/4 = 50.74$ Å^3). The calculated permittivity is 10.96, larger than the measured maximum value $\sim$ 9.91. Shannon's additive rule usually gives good estimation for low permittivity materials and it is worth believing that the real permittivity of MoO_3 is around 11, which is 45 % and 67 % larger than the traditional one here and reported value,[13] respectively.

Conclusions

MoO_3 can not be well densified by conventional sintering with a relative $\rho \sim$ 64.5% obtained at 680 °C giving a $\varepsilon_r \sim$ 7.58, a Qf $\sim$ 35,000 GHz and a TCF $\sim -$ 39 ppm/°C. Water-assisted cold sintering method increased the relative density of MoO_3 ceramic to $\sim$ 78 %, which was further improved to $\sim$ 83 % by the addition of $(NH_4)Mo_7O_{24} \bullet 4H_2O$. However, higher temperature annealing was still required to eradicate secondary phases and / or and increase Qf. Calculated ε_r of MoO_3 using Shannon's additive rule is $\sim$ 10.96, which is 10 % larger than that of the optimum cold sintered samples. Although relative ρ of MoO_3 did not achieve > 95 %, the methodology of introducing a cold sintering step for materials that are difficult to be sintered is adequately demonstrated.

ACKNOWLEDGEMENTS

Reference

(1) Sebastian, M. T.; Jantunen, H. Low Loss Dielectric Materials for LTCC Applications: A Review. Int. Mater. Rev. **2008**, 53, 57–90.

(2) Zhou, H.; Liu, X.; Chen, X.; Fang, L.; Wang, Y. $ZnLi_{2/3}Ti_{4/3}O_4$: A new low loss spinel microwave dielectric ceramic. J. Eur. Ceram. Soc. **2012**, 32, 261–265.

(3) Zhang, Y. D.; Zhou, D. Pseudo phase diagram and microwave dielectric Properties of Li_2O-MgO-TiO_2 ternary system. J. Am. Ceram. Soc. **2016**, 99, 3645–3650.

(4) Pang, L. X.; Zhou, D.; Qi, Z. M.; Liu, W. G.; Yue, Z. X.; Reaney, I. M.; Structure–property relationships of low sintering temperature scheelite-structured $(1-x)BiVO_4$–$xLaNbO_4$ microwave dielectric ceramics, J. Mater. Chem. C **2017**, 5, 2695–2701.

(5) Pang, L. X.; Zhou, D.; Li, W. B.; Yue, Z. X. High quality microwave dielectric ceramic sintered at extreme-low temperature below 200 and co-firing with base metal, J. Eur. Ceram. Soc. **2017**, 37, 3073–3077.

(6) Zhou, D.; Pang, L. X.; Wang, D. W.; Li, C.; Jin, B. B.; Reaney, I. M. High permittivity and low loss microwave dielectrics suitable for 5G resonators and low temperature co-fired ceramic architecture, J Mater. Chem. C **2017**, 5, 10094–10098.

(7) Zhou, D.; Guo, D.; Li, W. B.; Pang, L. X.; Yao, X.; Wang, D. W.; Reaney, I. M. Novel temperature stable high-ε_r microwave dielectrics in the Bi_2O_3–TiO_2–V_2O_5 system, J. Mater. Chem. C **2017**, 4, 5357–5362.

(8) Sebastian, M. T.; Wang, H.; Jantunen, H. Low temperature co-fired ceramics with ultra-low sintering temperature: A review. Current Opinion Solid State Mater. Sci. **2016**, 20, 151–170.

(9) Kwon, D. K.; Lanagan, M. T.; Shrout. T. R. Microwave dielectric properties and

low-temperature co-firing of $BaTe_4O_9$ with aluminum metal electrode. J. Am. Ceram. Soc. **2005**, 88, 3419–3422.

(10) Pang, L. X.; Zhou, D. Modification of $NdNbO_4$ microwave dielectric ceramic by Bi substitutions, J. Am. Ceram. Soc. **2019**, 00, 1–5. https://doi.org/10.1111/jace.16290.

(11) Joseph, N.; Varghese, J.; Siponkoski, T.; Teirikangas, M.; Sebastian, M. T.; Jantunen, H. Glass-free $CuMoO_4$ ceramic with excellent dielectric and thermal properties for ultralow temperature co-fired ceramic applications. ACS Sustainable Chem. Eng. **2016**, 4, 5632–5639.

(12) Zhou, D.; Pang, L. X.; Qi, Z. M.; Jin, B. B.; Yao, X. Novel ultra-low temperature co-fired microwave dielectric ceramic at 400 degrees and its chemical compatibility with base metal, Sci. Rep. **2014**, 4, 5980

(13) Varghese, J.; Siponkoski, T.; Nelo, M.; Sebastian, M. T.; Jantunen, H. Microwave dielectric properties of low-temperature sinterable α-MoO_3, J. Eur. Ceram. Soc. **2018**, 38, 1541–1547.

(14) Zhou, D.; Randall, C. A.; Wang, H.; Pang, L. X.; Yao, X. Microwave dielectric ceramics in Li_2O–Bi_2O_3–MoO_3 system with ultra-low sintering temperatures, J. Am. Ceram. Soc. **2010**, 93, 1096–1100.

(15) Sitepu, H.; O'Connor, B. H.; Li D. Comparative evaluation of the March and generalized spherical harmonic preferred orientation models using X-ray diffraction data for molybdate and calcite powders, J. Appl. Crys. **2005**, 38, 158–167.

(16) Leisegang, T.; Levin, A. A.; Walter, J.; Meyer, D. C. In situ X-ray analysis of MoO_3 reduction, Cryst. Res. Technol. **2005**, 40, 95–105.

(17) Guo, J.; Baker, A. L.; Guo, H.; Lanagan, M.; Randall, C. A. Cold sintering process: A new era for ceramic packaging and microwave device development, J. Am. Ceram. Soc. 2016, 100, 669–677.

(18) Guo, J.; Guo, H.; Baker, A. L.; Lanagan, M. T.; Kupp, E. R.; Messing, G. L.; Randall, C. A. Cold sintering: a paradigm shift for processing and integration of ceramics, Angew. Chem. Int. Edit. **2016**, 55, 11457–11461.

(19) Kahari, H.; Teirikangas, M.; Juuti, J.; Jantunen, H. Improvements and Modifications to Room-Temperature Fabrication Method for Dielectric Li_2MoO_4 ceramics, J. Am. Ceram. Soc. **2015**, 98, 687–689.

(20) Kahari, H.; Teirikangas, M.; Juuti, J.; Jantunen, H. Dielectric Properties of Lithium Molybdate Ceramic Fabricated at Room Temperature, J. Am. Ceram. Soc. **2014**, 97, 3378–3379.

(21) Kahari, H.; Teirikangas, M.; Juuti, J.; Jantunen, H. Room-temperature fabrication of microwave dielectric Li_2MoO_4-TiO_2 composite ceramics, Ceram. Int. **2016**, 42, 11442–11446.

(22) Parsons, T.; Maita, V.; Lalli, C. A manual of chemical and biological methods for seawater analysis. **1984**, Oxford: Pergamon.

(23) Evans, H. T.; Gatehouse, B. M.; Leverett, P. Crystal Structure of the Heptamolybdate(VI) (paramolybdate) ion, $(Mo_7O_{24})^{6-}$, in the ammonium and potassium tetrahydrate salts, Cheminform, 1975, 505–514.

(24) Geng, D. Y.; Zhang, Z. D.; Zhang, M.; Li, D.; Song, X. P.; Hu, K. Y. Structure and surface characterization of alpha-MoO_3 whiskers synthesized by an oxidation process, Scripta Mater. **2004**, 50, 983–986.

(25) Phadungdhitidhada, S.; Mangkorntong, P.; Choopun, S.; Mangkorntong, N.; Wongratanaphisan, D. Synthesis of MoO_3 nanobelts by medium energy nitrogen ion implantation, Mater. Lett. **2011**, 65, 568–571.

(26) Phadungdhitidhada, S.; Mangkorntong, P.; Choopun, S.; Mangkorntong, N., Raman scattering and electrical conductivity of nitrogen implanted MoO_3 whiskers, Ceram. Int. **2008**, 34, 1121–1125.

(27) Benchrifa, R.; le Blanc, M.; de Pape, R. Synthesis and crystal structure of two polymorphs of $(NH_4)_2Mo_4O_{13}$, orthorhombic (o) and triclinic (t), Eur. J. Solid State Inor. Chem. **1989**, 26, 593–601.

(28) Shannon, R. D. Dielectric polarizabilities of ions in oxides and fluorides, J. Appl. Phys. **1993**, 73, 348–366.

(29) Choi, G. K.; Kim, J. R.; Yoon, S. H.; Hong, K. S. Microwave dielectric properties of scheelite (A = Ca, Sr, Ba) and wolframite (A = Mg, Zn, Mn) $AMoO_4$ compounds, J. Eur. Ceram. Soc. 2007, 27, 3063–3067.

(30) Rysselberghe, P. V. Remarks concerning the Clausius–Mossotti law, J. Phys. Chem. **1932**, 36, 1152–1155.

Figure Captions:

Fig. 1 a) Relative ρ, ε_r and Qf value of MoO_3 ceramics prepared via conventional sinteriing as a function of sintering temperature (640 ~ 740 ℃). b) Optical images of starting powdersand MoO_3 ceramic sintered at 680 ℃ / 2 h with its crystal structure inset.

Fig. 2 a) XRD patterns of the raw MoO_3 powders, natural and fractured surfaces of cold sintered MoO_3 ceramic at 150 ℃ for 0.5 h, and annealed sample 620 ℃. b) Optical and SEM images of the starting powders and cold sintered MoO_3 ceramics.

Fig. 3 a) Relative ρ, ε_r and b) Qf of the MoO_3 prepared via conventional and cold sintering methods as a function of sintering temperature.

Fig. 4 XRD patterns of the starting $(NH_4)_6Mo_7O_{24}\cdot 4H_2O$ powder, cold sintered MoO_3 ceramic with $(NH_4)_6Mo_7O_{24}\cdot 4H_2O$ (150 ℃ for 0.5 h) and a sample annealed at 600 ℃, and optical and SEM images of the starting powders and cold sintered MoO_3 ceramics.

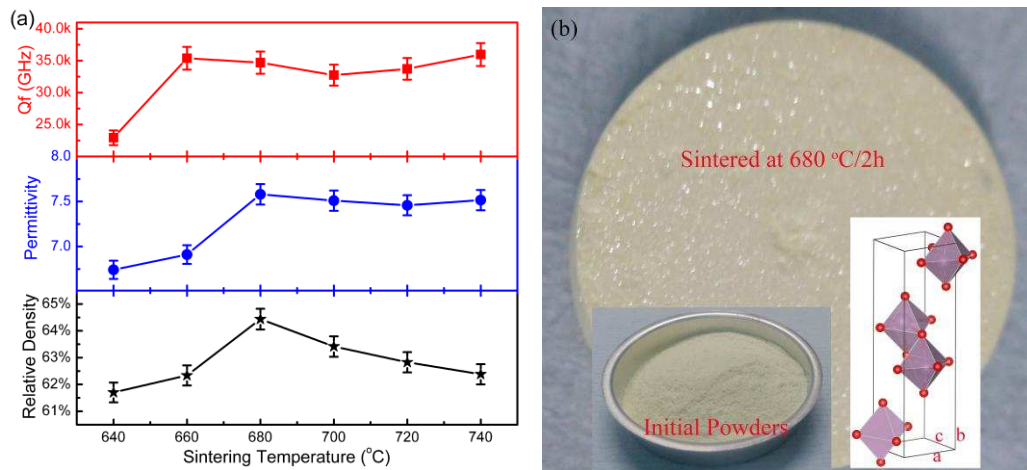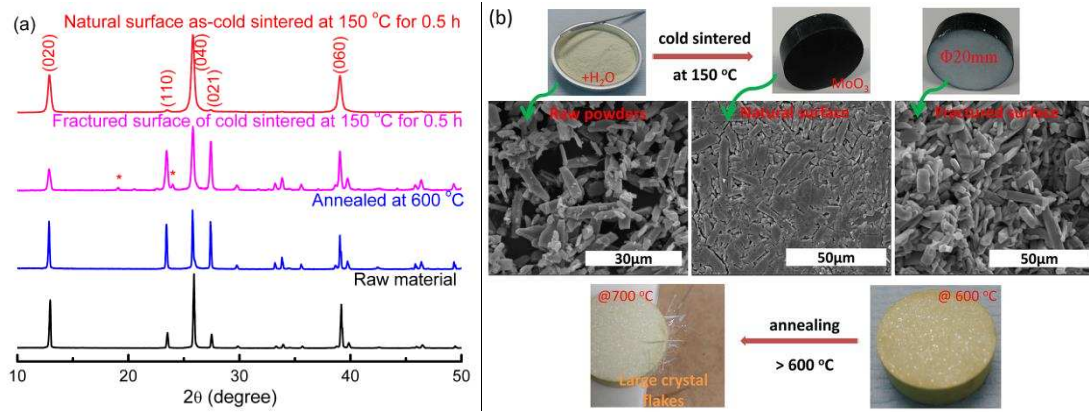Fig. 1 a) Relative ρ, ε_r and Qf value of MoO_3 ceramics prepared via conventional sinteriing as a function of sintering temperature (640 ~ 740 ^{o}C). b) Optical images of starting powdersand MoO_3 ceramic sintered at 680 ^{o}C / 2 h with its crystal structure inset.

Fig. 2 a) XRD patterns of the raw MoO_3 powders, natural and fractured surfaces of cold sintered MoO_3 ceramic at 150 ℃ for 0.5 h, and annealed sample 620 ℃. b) Optical and SEM images of the starting powders and cold sintered MoO_3 ceramics.
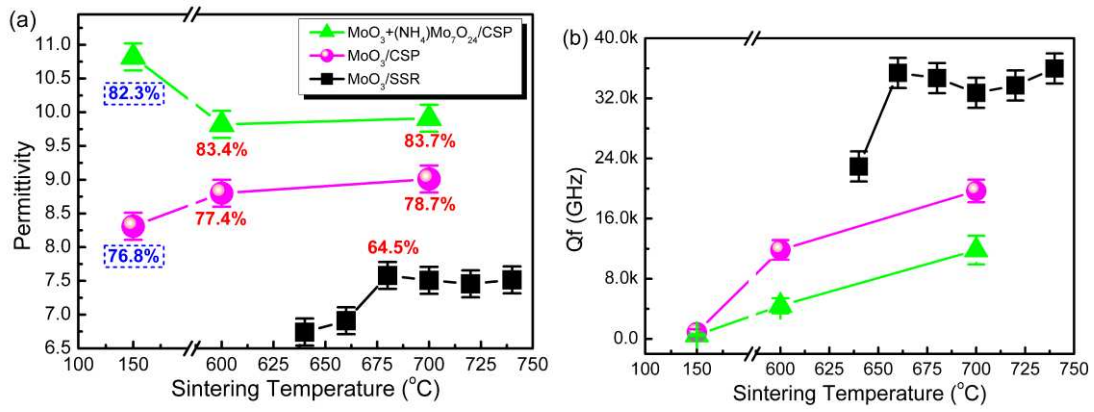
Fig. 3 a) Relative ρ, ε_r and b) Qf of the MoO$_3$ prepared via conventional and cold sintering methods as a function of sintering temperature.
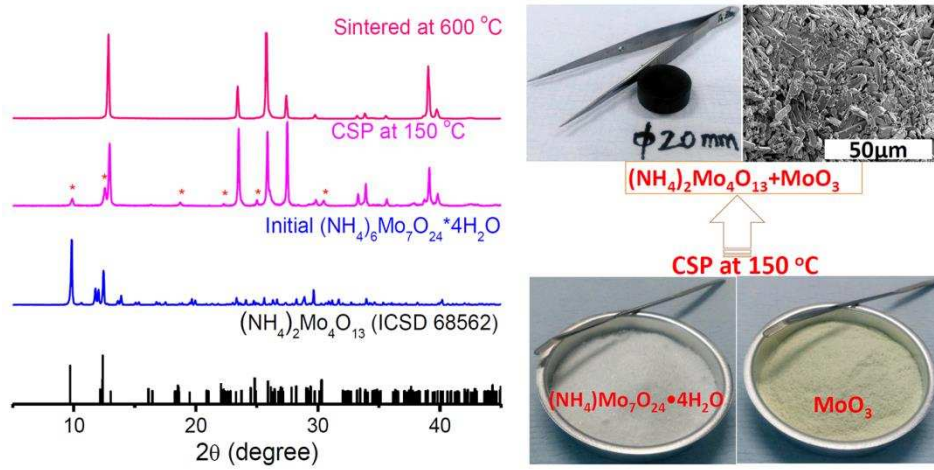
Fig. 4 XRD patterns of the starting $(NH_4)_6Mo_7O_{24} \cdot 4H_2O$ powder, cold sintered MoO_3 ceramic with $(NH_4)_6Mo_7O_{24} \cdot 4H_2O$ (150 ^{o}C for 0.5 h) and a sample annealed at 600 ^{o}C, and optical and SEM images of the starting powders and cold sintered MoO_3 ceramics.

For Table of Contents Only: MoO_3 ceramics can not be well densified via conventional solid state method and a low relative density ~ 64.5 % was obtained with a permittivity (ε_r) ~ 7.58. Cold sintering at 150 °C enhanced densification and give a relative ρ ~ 76.8 % and ε_r ~ 8.31. Addition of $(NH_4)_6Mo_7O_{24}\cdot4H_2O$ further improved densification to give a relative ρ ~ 83.7 % after annealing at 700 °C, resulting in a ε_r ~ 9.91.